Journal of Applied Sciences and Applications in Engineering

SCIVOLVE

Review Article

Open Access Full Text Article

Bio-Inspired Wing Designs for UAVs and Low Speed Aircraft

Ajayi Abiola Samuel[1]*, Elijah Effiong G. Osimene[2], Brian Cobb Hanrahan[3], Shokenu Emmanuel Segun[4], Bodude Ayoola David[5], Ajayi Eniola Isaac[6], Matthew Peace Ehigocho[7]

[1]Department of Computer Science, Texas Southern University, USA.
[2]Department of Aerospace Engineering, Air Force Institute of Technology, Kaduna, Nigeria.
[3]World Aerospace, Discovery Business Park, Cedar Park, Texas, USA.
[4]Department of System Engineering, African University of Science and Technology Nigeria.
[5]Department of Chemical Engineering. University of Strathclyde, Galsgow, UK.
[6]Department of Computer Science, Aptech Computer Insitute, Nigeria.
[7]Department of Aerospace Engineering, Air Force Institute of Technology, Kaduna, Nigeria.

Correspondence:
Ajayi Abiola Samuel
Department of Computer Science, Texas Southern University, USA.

Received: January 24, 2026; **Published:** February 23, 2026

How to cite this article:
Ajayi, A. S., Osimene, E. E. G., Hanrahan, B. C., Segun, S. E., David, B. A., Isaac, A. E., & Ehigocho, M. P. (2026). Bio-inspired wing designs for UAVs and low-speed aircraft. *Journal of Applied Sciences and Applications in Engineering, 2*(1), 1–11.

Abstract

The aviation industry is under increasing pressure to reduce fuel consumption and emissions, driving the search for innovative aerodynamic solutions. This study presents a numerical investigation of bio-inspired airfoils as alternatives to conventional designs for drag reduction and efficiency improvement in low-Reynolds-number applications relevant to UAVs and future commercial aircraft. Five airfoils were evaluated: three bio-inspired geometries (Albatross, Falcon, Owl) and two conventional baselines (Eppler 387 and NACA 4412). Simulations were performed using a steady-state Reynolds-Averaged Navier–Stokes (RANS) solver with the SST k–ω transition model at angles of attack of 3°, 6°, 9°, and 15°. Results show that the Albatross achieved the highest lift coefficients, making it optimal for high-payload and STOL missions, while the Owl exhibited the lowest drag, offering endurance advantages for surveillance and ISR applications. The Falcon generated limited lift but competitive drag reduction, indicating a niche role for high-speed operations. In contrast, Eppler 387 and NACA 4412 underperformed due to stronger adverse pressure gradients and early flow separation. Pressure and velocity contour analyses confirmed that bio-inspired geometries promoted smoother pressure recovery and delayed boundary-layer separation compared to conventional profiles. Overall, the study demonstrates that bio-inspired morphing-inspired airfoils provide measurable aerodynamic advantages over fixed conventional designs, supporting the broader objective of employing morphing winglets to enhance drag reduction and flight efficiency in next-generation aircraft.

Keywords: Bio-inspired airfoils, drag reduction, aerodynamic efficiency, UAV design, Reynolds number, CFD simulation, lift-to-drag ratio.

Introduction

The aviation industry is under increasing pressure to reduce fuel consumption and greenhouse gas emissions, making aerodynamic efficiency a central priority for manufacturers and operators. Among the available strategies, advances in wing design have consistently proven effective in improving aircraft performance. Xia (2024) demonstrated that aerodynamic modifications such as morphing winglets can significantly lower drag and enhance jetliner fuel efficiency, thereby supporting environmental sustainability. Similarly, Clements (2023) emphasized that incorporating morphing mechanisms into lifting surfaces can boost energy efficiency not only for conventional aircraft but also for advanced transport systems operating under challenging aerodynamic conditions. These findings underscore the importance of innovation in wing design for addressing both economic competitiveness and environmental responsibility.

Winglets have long been employed to mitigate induced drag by weakening wingtip vortices, with well-established benefits for lift-to-drag ratios and overall flight performance. However, conventional winglets remain limited by their fixed geometry, which is optimized for cruise conditions but fails to maximize efficiency during other flight phases such as takeoff, climb, and descent. As Özel, *et al*. (2020) noted, this inability to adapt to varying aerodynamic environments restricts the potential aerodynamic gains of static devices.

Morphing winglets have emerged as a promising solution to these challenges. By actively adjusting their geometry during

flight, they allow performance optimization across multiple aerodynamic regimes. Eguea *et al*. (2021) demonstrated that camber morphing winglets not only reduce drag but also reshape vortex structures, delivering higher efficiency than conventional designs. Despite these advances, a clear research gap remains: few comparative CFD studies have directly analyzed morphing and traditional winglets under identical flight conditions. To address this gap, the present study numerically investigates bio-inspired morphing winglets to assess their potential in reducing drag and enhancing efficiency in UAVs and low-speed aircraft, building on aerodynamic principles and innovations in adaptive system design (Samuel *et al*., 2025).

Literature Review

Improving aerodynamic efficiency has long been a focus of aircraft design, particularly in response to the growing need for fuel savings and emission reduction. Winglets have been widely adopted in commercial aviation as passive devices that reduce induced drag by mitigating wingtip vortices, leading to measurable improvements in performance (Gavrilović *et al*., 2015). While conventional winglets provide clear efficiency gains, their fixed geometry restricts optimization to a narrow range of flight conditions. To address this limitation, researchers have investigated morphing winglet concepts capable of adapting their geometry during different phases of flight, such as takeoff, climb, cruise, and landing (Ursache *et al*., 2007). This adaptability has been identified as a pathway to achieving performance improvements beyond those offered by static winglets.

Several studies have examined the aerodynamic benefits of camber morphing winglets. Eguea *et al*. (2020) demonstrated that incorporating a camber morphing concept on a business jet improved fuel efficiency by altering the pressure distribution at the wingtip. Their findings were extended by Eguea *et al*. (2021), who showed that such morphing mechanisms also influenced tip vortex structures, thereby reducing drag and contributing to more favorable aerodynamic performance. These studies suggest that morphing winglets not only mitigate induced drag more effectively than static devices but also improve wake flow behavior, offering advantages for real flight operations.

Beyond drag reduction, research has highlighted the potential of morphing winglets to enhance load control and aeroelastic performance. Liauzun *et al*. (2018) explored adaptive winglet concepts and found improvements in aeroelastic stability, which is critical for maintaining structural safety under dynamic conditions. Complementing this, Wang and Yuan (2024) reviewed structural design approaches, noting the need to balance aerodynamic performance gains with the mechanical demands of morphing mechanisms. Optimization research by Rajabi and Jahangirian (2025) further emphasized the potential of designing morphing winglets to perform effectively across multiple flight phases, representing an advancement toward practical integration in next-generation commercial aircraft.

The literature also situates morphing winglets within a broader trend of adaptive and sustainable engineering solutions. Popov *et al*. (2020) reported measurable fuel efficiency improvements from adaptive wing technologies, while Kaygan (2020) confirmed that morphing winglets outperform traditional fixed designs in aerodynamic performance analyses. Moreover, research outside the aviation field highlights how adaptive technologies are increasingly applied to improve system efficiency and control in diverse domains, such as traffic management through RFID-enabled monitoring (Segun *et al*., 2023). Collectively, these studies indicate that morphing winglets hold strong promise for meeting future efficiency requirements in aviation.

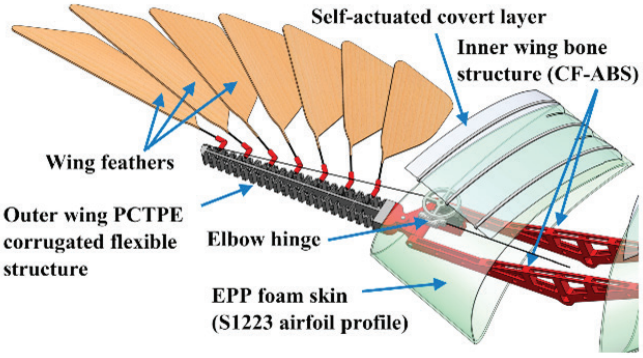

Figure 1: 3D-Printed Corrugated Sweep-Morphing Wing and Feather-Expansion Tail Mechanism for UAVs (adapted from "3D-Printed Bio-Inspired Mechanisms for Bird-like Morphing Drones" by (Bishay *et al*., 2023)).

Figure 1 illustrates a bio-inspired morphing wing and tail design that combines corrugated sweep morphing with feather-like expansion, enabling adaptive geometry during different phases of flight (Bishay *et al*., 2023). This concept aligns with the structural review by Wang and Yuan (2024), who emphasized that morphing configurations depend on flexible materials and innovative actuation mechanisms to balance aerodynamic efficiency with structural integrity. By dynamically altering camber, sweep, or deflection, such morphing systems reduce induced drag and improve lift distribution, particularly beneficial for UAVs and low-speed aircraft operating at low Reynolds numbers (Xia, 2024). Optimization studies further confirm that designs like those shown in Figure 1 can be tuned across multiple mission segments from takeoff to cruise and landing ensuring consistent aerodynamic performance (Rajabi & Jahangirian, 2025). More broadly, the integration of adaptability into airfoil and wing structures represents a next-generation approach in aerospace engineering, comparable to advanced predictive modeling used in other engineering domains to optimize complex flow systems (Ajayi *et al*., 2024).

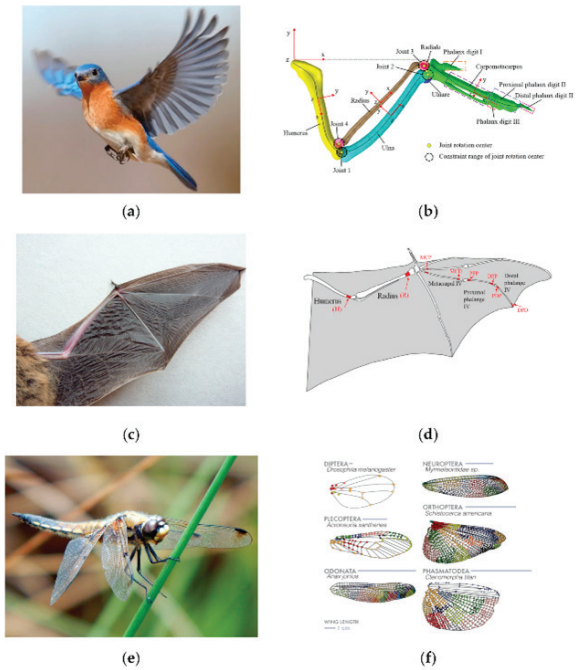

Figure 2: Avian Wing Anatomy Schematic Demonstrating Natural Morphing Structures (bones, feathers, articulated joints) Adapted from "Bioinspired Morphing in Aerodynamics and Hydrodynamics:

Engineering Innovations for Aerospace and Renewable Energy" (Shahid *et al*., 2025).

Figure 2 presents a schematic of avian wing anatomy, highlighting natural morphing features such as flexible bones, feathers, and articulated joints that inspire compliant wingtip designs for UAVs and low-speed aircraft (Shahid *et al*., 2025). These biological mechanisms parallel engineering concepts where corrugated and compliant structures enable continuous deformation without hinges, reducing structural complexity while maintaining aerodynamic adaptability. As emphasized by Wang and Yuan (2024), morphing systems depend on flexible materials and advanced actuation strategies to balance efficiency and structural integrity. Such compliant configurations allow redistribution of aerodynamic loads, delaying flow separation and enhancing stability across varying flight regimes (Xia, 2024). Optimization studies further demonstrate that compliant structures can be tuned to sustain favorable aerodynamic characteristics across multiple mission phases (Rajabi & Jahangirian, 2024). Beyond aerodynamics, the innovative use of compliant panels reflects a broader engineering principle: employing flexible yet predictable material behaviors to improve system performance, as seen in computational models of biological and environmental systems (Ajayi *et al*., 2024; Fasasi *et al*., 2024).

Despite these advances, the literature highlights a clear gap in comprehensive comparative analyses of bio-inspired wings and conventional airfoils under identical CFD conditions across multiple flight regimes. Most studies focus either on aerodynamic efficiency or structural feasibility, but few evaluate their integrated performance under realistic operational scenarios. To address this gap, the present study numerically investigates bio-inspired wings against conventional designs, emphasizing drag reduction, lift-to-drag ratio improvements, and overall flight efficiency in UAV and low-speed aircraft.

Fasasi *et al* (2024) introduced an expert system for predicting aircraft failure causes and recommending remedies, underscoring the role of computational intelligence in aerospace. While their work targeted safety and reliability, similar approaches can be extended to performance optimization, such as anticipating aerodynamic inefficiencies. This perspective strengthens the case for bio-inspired wing designs, where adaptive morphologies combined with intelligent control can enhance both efficiency and operational safety.

Recent research further demonstrates that aerodynamic efficiency can be improved through refinements in winglet and camber morphing strategies. Yusoff *et al*. (2022) showed that multi-winglet configurations reduce induced drag on conventional airfoils such as the NACA23015, confirming the significance of wingtip modifications. Building on this, Madani *et al*. (2025) employed CFD to study winglet cant angles, revealing not only aerodynamic benefits but also aeroacoustic trade-offs that must be considered in practice. Reist *et al*. (2022) extended the discussion to variable camber using existing control surfaces, proving that drag reduction can be achieved without fundamentally altering aircraft structures, thus offering operational feasibility for integration. Parallel advances in thermal-fluid sciences, such as Ajayi *et al*. (2024) condensation heat transfer and pressure drop model, further underscore a common engineering principle: optimizing system performance under complex flow conditions.

Collectively, these studies show that while wing evolution and morphing mechanisms deliver measurable aerodynamic gains, the key challenge lies in embedding these designs within robust, multidisciplinary frameworks that balance drag reduction, acoustic impacts, and practical feasibility for next-generation aircraft.

Methodology

The aerodynamic analysis was carried out on five distinct airfoils representing both bio-inspired and conventional design philosophies. The bio-inspired group included the Albatross (high aspect ratio, high camber), Falcon (low camber, high-speed profile), and Owl (serrated leading edge with noise-abatement features). These were compared with two well established conventional airfoils: the Eppler 387, a low-Reynolds number optimized section, and the NACA 4412, a widely studied cambered airfoil that serves as a historical baseline. This combination of geometries enabled a comprehensive evaluation of bio-inspired versus traditional designs under identical computational conditions.

The computational fluid dynamics (CFD) simulations were performed using a pressure-based, steady state Reynolds-Averaged Navier-Stokes (RANS) solver in ANSYS Fluent. The Shear Stress Transport (SST) k–ω transition model was chosen for its ability to capture laminar-to-turbulent transition and accurately predict flow separation under adverse pressure gradients, which is critical in low-Reynolds number flows. A two-dimensional C-mesh topology was constructed, refined with a minimum of 20 inflation layers, and calibrated to achieve $y+ << 1$ for accurate viscous sublayer resolution. Grid independence was confirmed through mesh refinement studies. The boundary conditions included a uniform velocity inlet, pressure outlet, and no-slip wall on the airfoil surfaces. Simulations were conducted at angles of attack (AoA) of 3°, 6°, 9°, and 15°, representing both typical operational conditions and near-stall scenarios.

The analysis focused on extracting lift (CL) and drag (CD) coefficients across the tested AoAs, along with flow field diagnostics using pressure and velocity contours. The results revealed unconventional aerodynamic behaviors characteristic of low-Reynolds-number regimes, including laminar separation bubbles and premature stall. The Albatross demonstrated superior lift retention at higher AoAs, while the Owl exhibited the lowest drag, making it the most favorable for endurance-focused missions. Pressure contour analysis showed that bio-inspired profiles maintained smoother pressure gradients, reducing separation risks compared to conventional airfoils. Velocity contours confirmed streamlined acceleration and delayed boundary-layer separation in the bio-inspired designs. These diagnostics provided insights into the mechanisms behind the improved lift-to-drag ratios of the Albatross and Owl airfoils, positioning them as strong candidates for UAV applications where payload or endurance are critical.

Results

The numerical simulations produced a detailed aerodynamic performance comparison across the five investigated airfoils. Table 1 presents the computed lift (CL) and drag (CD) coefficients at angles of attack of 3°, 6°, 9°, and 15°. The results demonstrate the distinct aerodynamic behavior of bio-inspired versus conventional airfoils, highlighting the effectiveness of bio-inspired designs in low Reynolds number regimes.

Table 1. Lift (CL) and drag (CD) coefficients for bio-inspired and conventional airfoils at different angles of attack.

Airfoil	3° AoA	6° AoA	9° AoA	15° AoA
Albatross	CL: 0.302	CL: 0.103	CL: 0.109	C_L: 0.113
	CD: 0.045	CD: 6.89e-4	CD: -0.0013	C_D: -0.0037
Falcon	CL: 0.120	CL: 0.056	CL: 0.063	CL: 0.069
	CD: 0.039	CD: 8.76e-4	CD: -5.63e-4	CD: -0.0023
Owl	CL: 0.144	CL: 0.068	CL: 0.075	CL: 0.079
	CD: 0.023	CD: 0.0012	CD: -2.03e-4	CD: -0.0017
Eppler 387	CL: 0.209	CL: 0.083	CL: 0.089	CL: 0.095
	CD: 0.033	CD: 3.21e-4	CD: -0.0015	CD: -0.0036
NACA 4412	CL: 0.233	CL: 0.078	CL: 0.083	CL: 0.086
	CD: 0.049	CD: 0.0019	CD: 3.21e-4	CD: -0.0015

Table 1 presents the lift (Cl) and drag (Cd) coefficients of the bio-inspired and conventional airfoils at different angles of attack (AoA). At 3° AoA, all airfoils achieve their maximum lift, with the albatross generating the highest Cl (0.302), making it best suited for payload-intensive and short takeoff and landing (STOL) missions. The conventional Eppler 387 and NACA 4412 record moderate lift values (0.21 and 0.23, respectively), though accompanied by relatively higher drag, while the falcon and owl produce the lowest lift (~0.12–0.14). Drag is also highest at 3°, with the NACA 4412 showing the largest Cd (0.049) and the owl the lowest (0.023), positioning the owl as the most efficient airfoil for endurance-focused missions where reduced drag is critical. As AoA increases to 6° and beyond, drag decreases sharply to near-zero or slightly negative values, reflecting improved aerodynamic efficiency, while lift stabilizes at reduced levels compared to 3°. Overall, the albatross demonstrates superior lift performance across all AoAs, the owl consistently minimizes drag, and the falcon though less effective in lift shows potential for specialized high-speed applications.

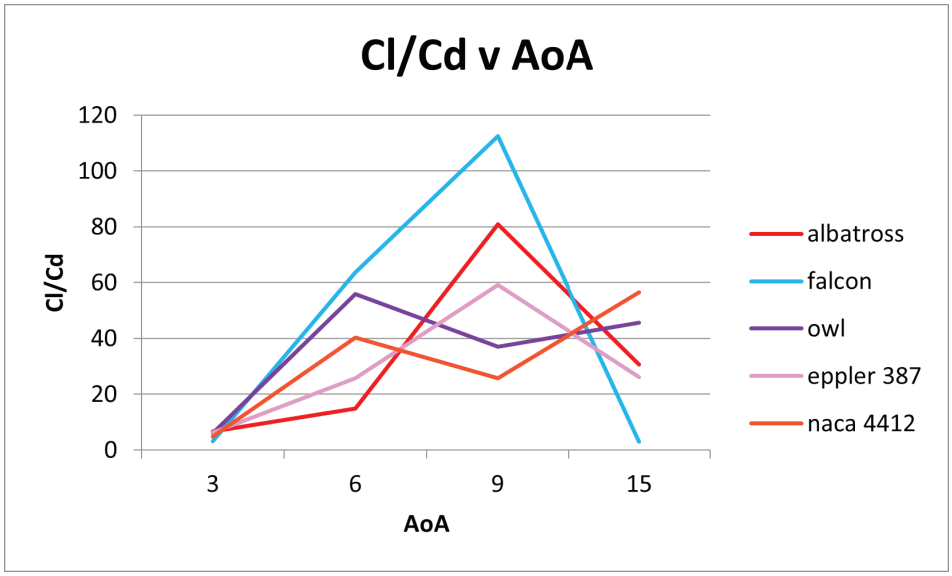

Figure 3: Variation of Lift-to-Drag Ratio (Cl/Cd) with Angle of Attack for Bio-Inspired and Conventional Airfoils

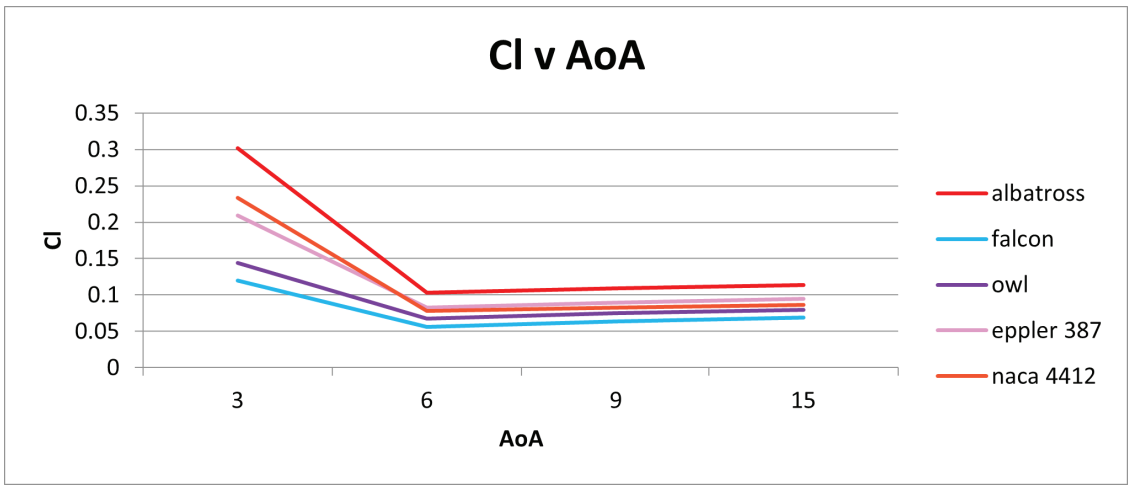

Figure 4: Variation of Lift Coefficient (Cl) with Angle of Attack for Bio-Inspired and Conventional Airfoils

Figure 3 illustrates the variation of lift-to-drag ratio (Cl/Cd) with angle of attack (AoA) for the five airfoils tested. This show that bio-inspired airfoils generally outperform conventional designs, particularly in low-Reynolds number conditions. The Falcon achieves the highest peak efficiency at 9° AoA, highlighting its suitability for specialized high-speed missions with minimal drag penalties. The Albatross demonstrates consistently strong Cl/Cd values, confirming its advantage for payload intensive or short takeoff and landing (STOL) operations where high lift is critical. The Owl maintains stable efficiency across AoAs, reinforcing its role in endurance-focused missions. In contrast, conventional airfoils (Eppler 387 and NACA 4412) show lower and less stable ratios, reflecting earlier flow separation and reduced adaptability.

Figure 4 shows the variation of lift coefficient (Cl) with angle of attack (AoA) for the bio-inspired and conventional airfoils. At a low AoA of 3°, all models achieve their maximum lift, with the albatross wing producing the highest Cl (0.3), confirming its superior lift-generating capability under low-Reynolds-number conditions. Conventional airfoils (Eppler 387 and NACA 4412) follow with moderate lift values, while the falcon and owl exhibit the lowest Cl (0.12–0.15), indicating limited lift potential. As AoA increases to 6°, all airfoils experience a sharp reduction in Cl, reflecting early onset of stall or boundary layer separation. Beyond 6°, Cl recovers gradually up to 15°, but none of the designs regain the initial lift achieved at 3°. This trend highlights the albatross as the most effective bio-inspired wing for high-lift missions, supporting the study's objective of identifying optimal designs for UAVs and low-speed aircraft.

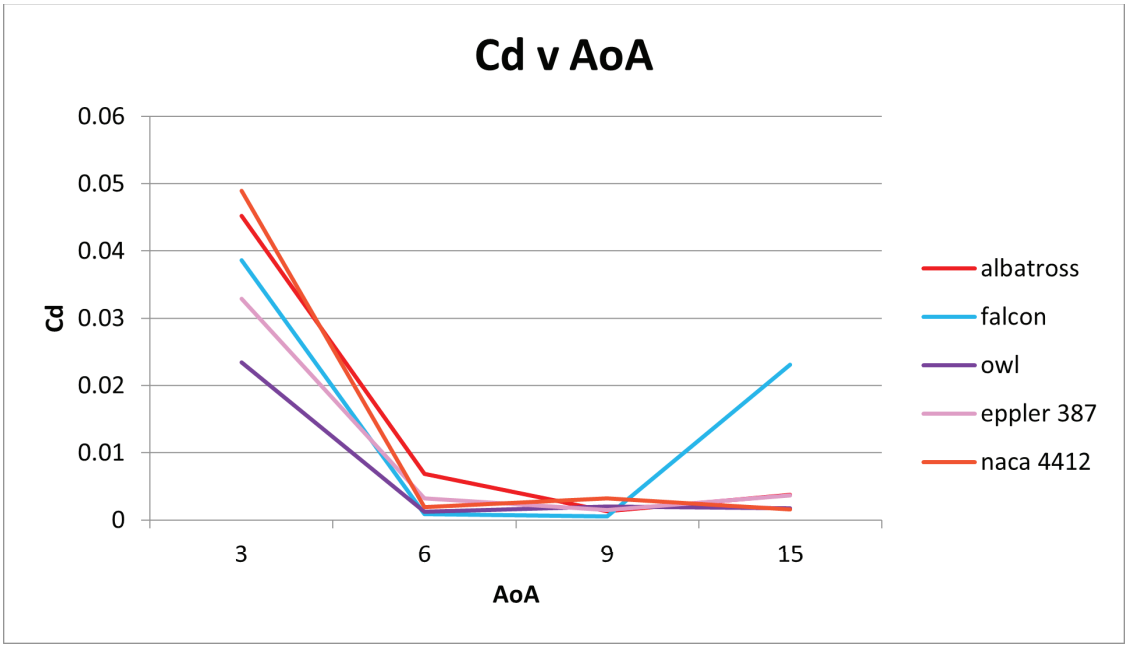

Figure 5: Variation of Drag Coefficient (Cd) with Angle of Attack for Bio-Inspired and Conventional Airfoils

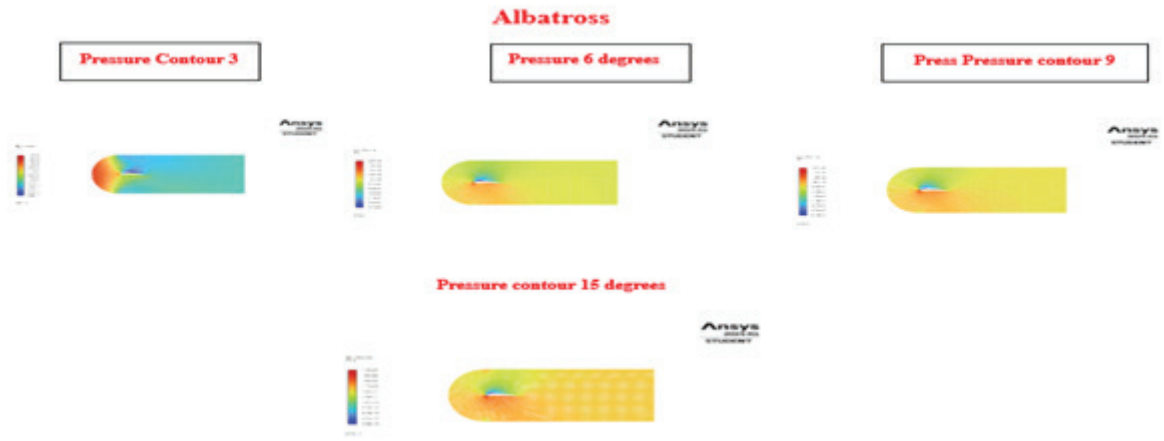

Figure 6. Pressure contours for the Albatross at selected angles of attack (3°, 6°, 9°, 15°).

Figure 5 illustrates the variation of drag coefficient (Cd) with angle of attack (AoA) for bio-inspired and conventional airfoils. At a low AoA of 3°, all designs record their highest drag, with the albatross and NACA 4412 reaching values around 0.05, while the owl demonstrates superior aerodynamic efficiency with the lowest Cd (0.02). As the AoA increases to 6°, drag drops sharply across all models, approaching near-zero values, which reflects improved aerodynamic performance at moderate incidence angles. From 6° to 9°, Cd remains consistently low and stable, indicating sustained drag reduction across both bio-inspired and conventional profiles.

At 15°, the falcon experiences a noticeable rise in drag compared to the others, which maintain low values. These results confirm that most bio-inspired and conventional airfoils achieve minimal drag in the mid-range AoAs, with the owl showing the greatest efficiency and the falcon losing performance at higher AoA.

Figure 6. illustrate the pressure contours for the Albatross at selected angles of attack (3°, 6°, 9°, 15°).

The Albatross airfoil maintains smooth pressure recovery with reduced adverse gradients across all AoAs. This explains its superior lift performance and delayed separation behavior. Even at 15°, the contours indicate sustained pressure differentials, making it suitable for high-lift missions.

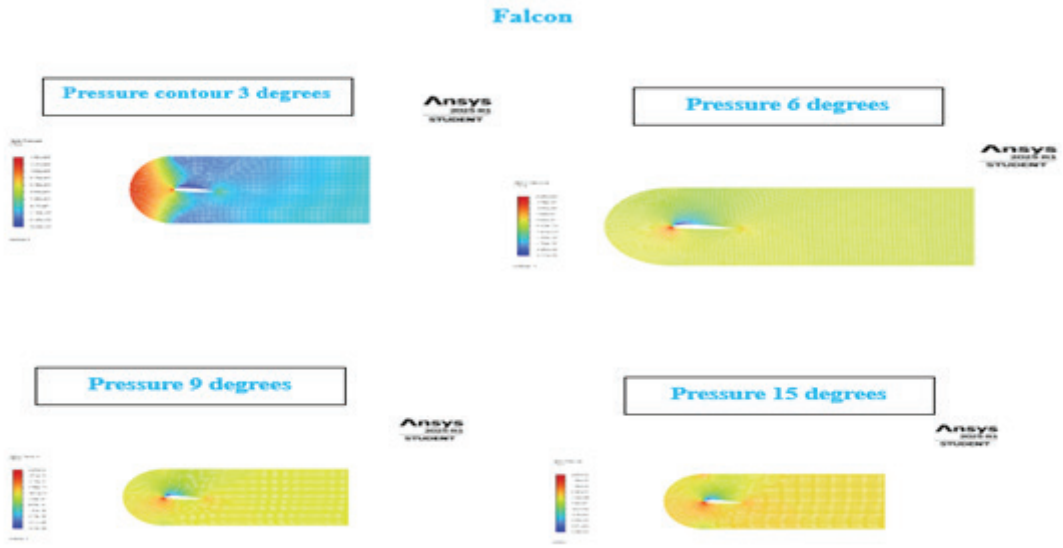

Figure 7. Pressure contours for Falcon airfoils at selected angles of attack (3°, 6°, 9°, 15°).

Figure 7 also show the pressure contours for Falcon airfoils at selected angles of attack (3°, 6°, 9°, 15°).

The Falcon exhibits weaker suction peaks and steeper gradients, causing earlier separation under increasing AoA. This limits its lift generation compared to other bio-inspired designs. Its contour patterns align with its specialization for low-drag, high-speed flight.

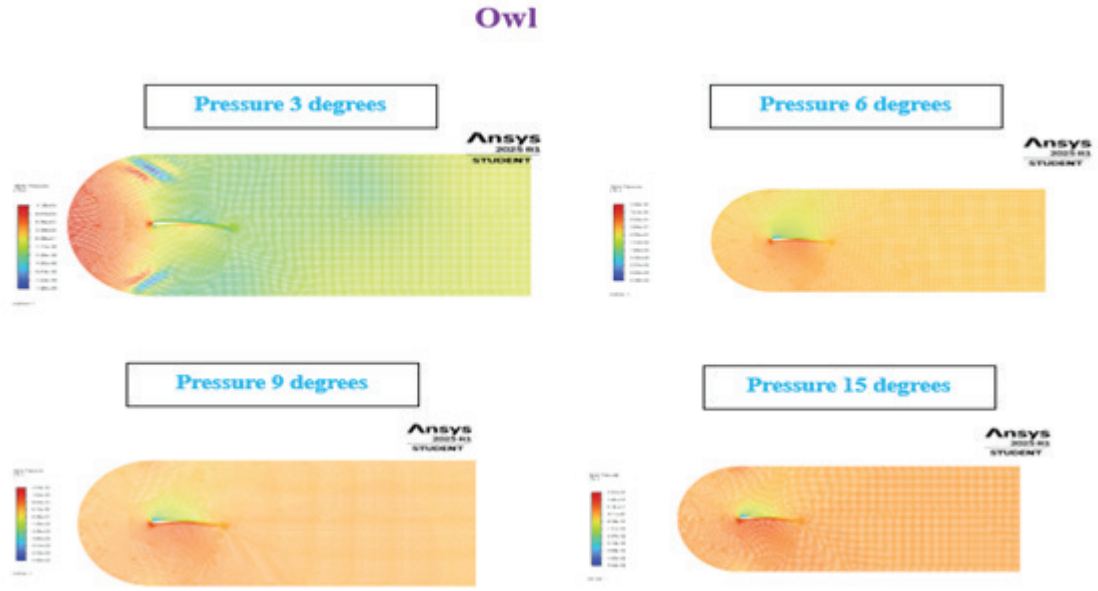

Figure 8. Pressure contours for Owl airfoils at selected angles of attack (3°, 6°, 9°, 15°).

Figure 8 show the pressure contours for Owl airfoils at selected angles of attack (3°, 6°, 9°, 15°).

The Owl shows a stable and gradual pressure recovery, especially at lower AoAs, with serrated leading edges helping to delay flow separation. This produces low drag while maintaining moderate lift. The contours confirm its role as an endurance optimized airfoil.

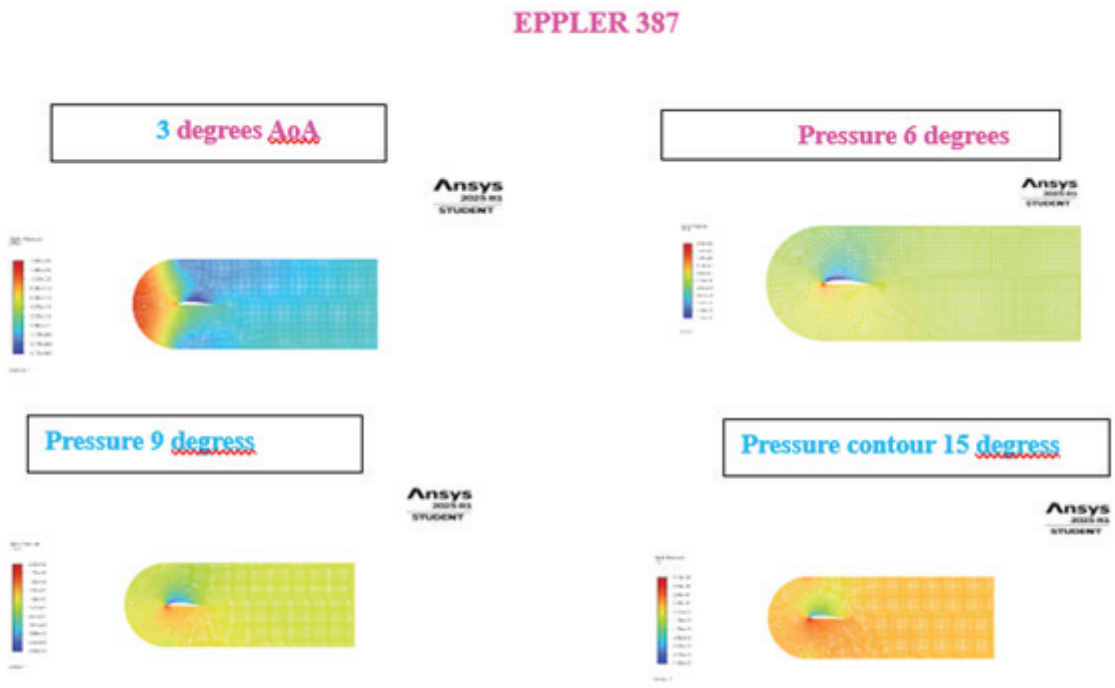

Figure 9. Pressure contours at different angles of attack (3°, 6°, 9°, 15°) for Eppler 387.

Figure 9 illustrate the pressure contours at different angles of attack (3°, 6°, 9°, 15°) for Eppler 387.

The Eppler 387 displays relatively sharp suction peaks, which initially provide lift but result in unstable recovery at higher AoAs. The contours indicate susceptibility to flow separation beyond moderate angles. This reduces efficiency compared to bio-inspired designs.

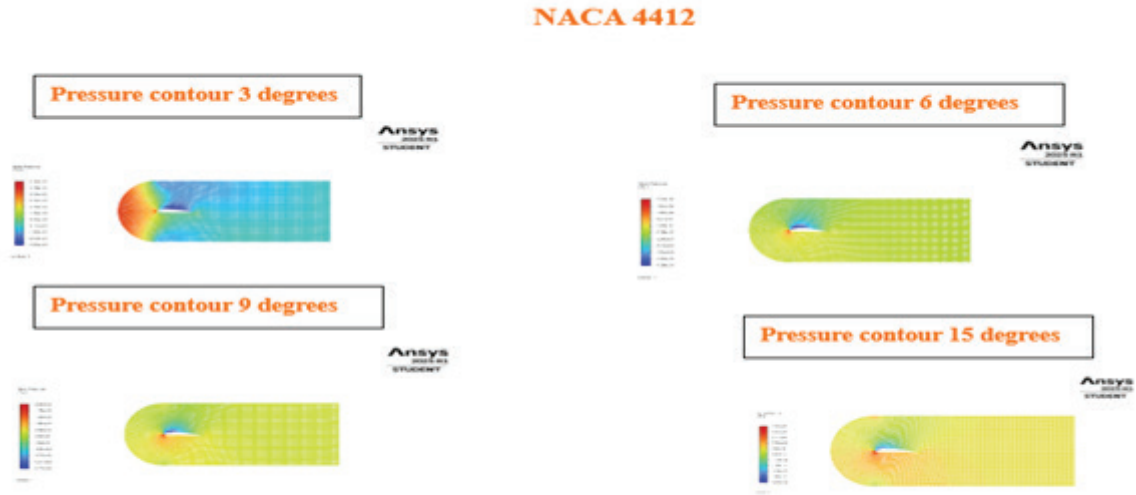

Figure 10. Pressure contours at different angles of attack (3°, 6°, 9°, 15°) for NACA 4412.

Figure 10 show the pressure contours at different angles of attack (3°, 6°, 9°, 15°) for NACA 4412.

The NACA 4412 shows strong pressure gradients and early flow detachment, particularly as AoA increases. This explains its consistently higher drag and reduced aerodynamic efficiency. Its contours highlight why conventional designs underperform at low Reynolds numbers.

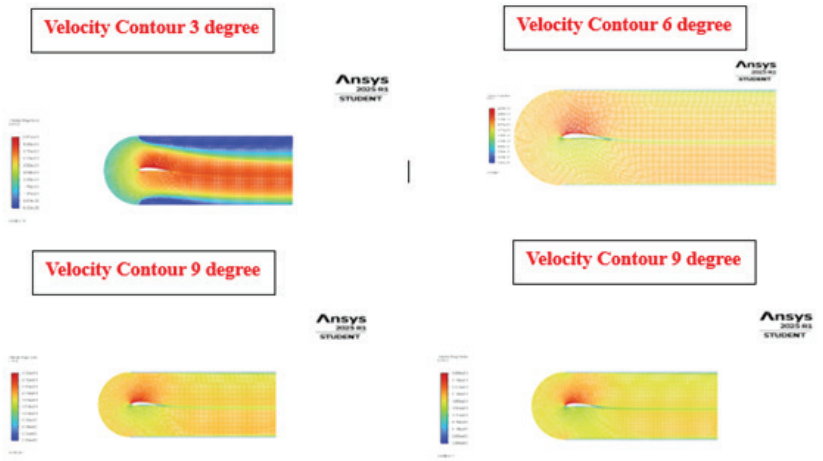

Figure 11. Velocity contours for the Albatross airfoil at selected angles of attack (3°, 6°, 9°, 15°).

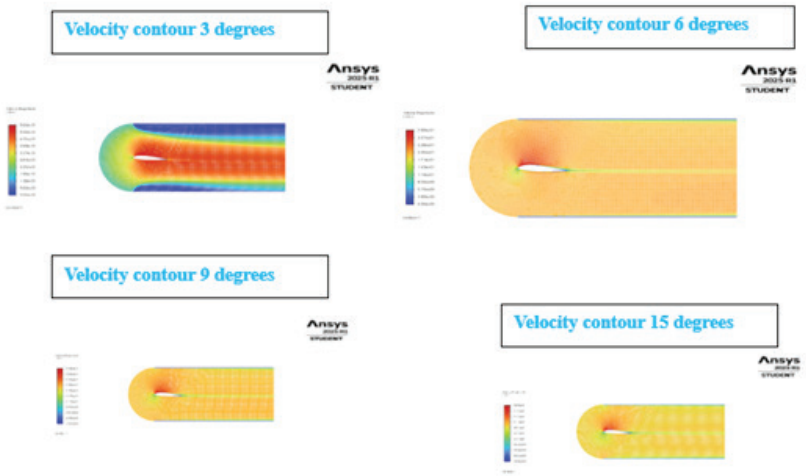

Figure 12. Velocity contours for the Falcon airfoil at selected angles of attack (3°, 6°, 9°, 15°).

Complementing the pressure analysis, the velocity distributions provide further insight into boundary layer behavior. Figure 11 shows that the Albatross supports high velocity over the suction surface with minimal reversed-flow regions, consistent with its superior lift.

In contrast, Figure 12 demonstrates that the Falcon produces lower velocities and larger recirculation areas at higher AoAs, aligning with its low lift capability.

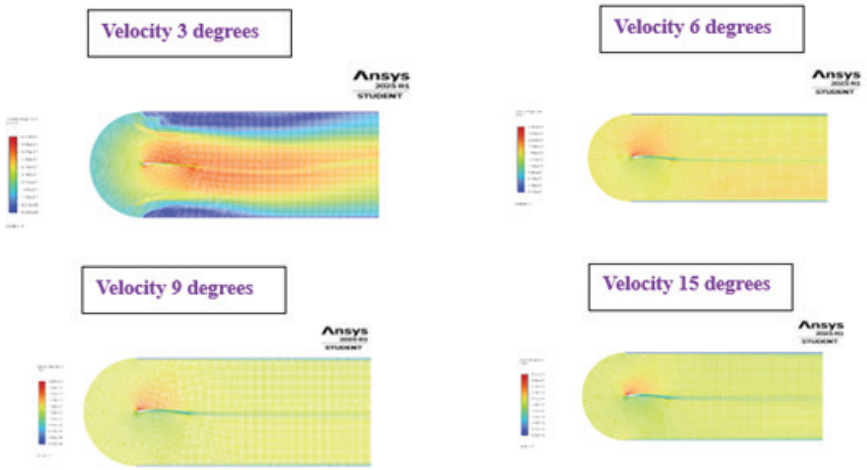

Figure 13. Velocity contours for the Owl airfoil at selected angles of attack (3°, 6°, 9°, 15°).

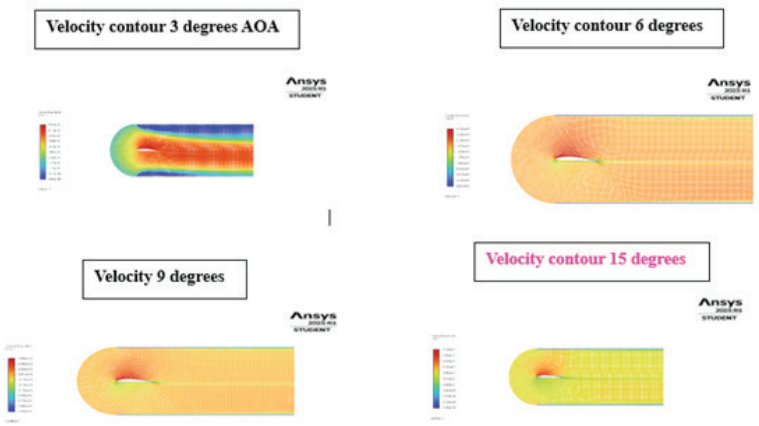

Figure 14. Velocity contours for the Eppler 387 airfoil at selected angles of attack (3°, 6°, 9°, 15°).

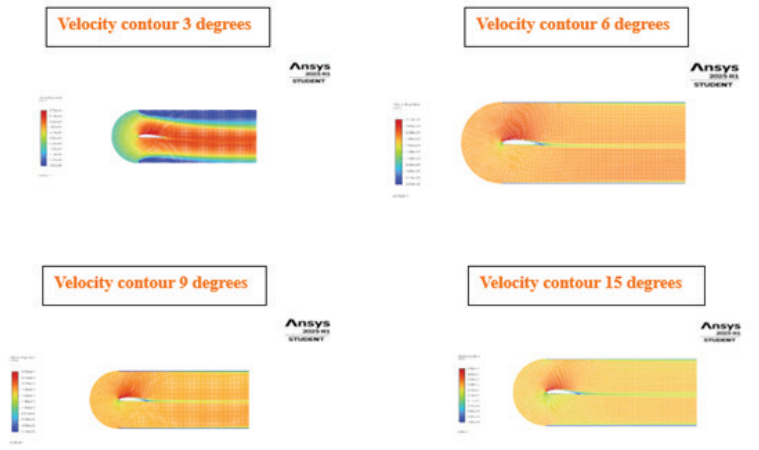

Figure 15. Velocity contours for the NACA 4412 airfoil at selected angles of attack (3°, 6°, 9°, 15°).

Figure 13 illustrates the velocity contours for the Owl, where streamlined acceleration and delayed separation are evident. The serrated leading edge promotes boundary layer reattachment, which explains the Owl's low drag and stable aerodynamic behavior. Conversely, Figure 14 shows that Eppler 387 suffers from early boundary layer breakdown, while Figure 15 highlights significant separation and reversed flow for the NACA 4412, both of which account for their reduced efficiency.

The CFD analysis revealed distinct aerodynamic behaviors across the five airfoils, with bio-inspired designs outperforming conventional ones under low Reynolds-number conditions. The Albatross consistently achieved the highest lift coefficients, maintaining aerodynamic performance even at higher angles of attack, making it ideal for payload-intensive or STOL UAV operations. The Owl demonstrated the lowest drag values and smoother flow characteristics, confirming its suitability for endurance and ISR missions where long flight times are essential. The Falcon showed efficiency in drag reduction but limited lift generation, restricting its utility to specialized high-speed missions. In contrast, conventional airfoils, particularly the NACA 4412, suffered from stronger adverse pressure gradients, early flow separation, and higher drag, which led to consistently poorer performance. These results provide strong evidence that bio-inspired morphing-inspired geometries can enhance UAV aerodynamic efficiency compared to traditional sections.

Conclusion

This study provides actionable insights for UAV and aircraft designers by identifying airfoil profiles best suited for different mission requirements. The Albatross airfoil is optimal for high-payload and STOL operations due to its superior lift, enabling heavier take-off weights, shorter runway requirements, and enhanced low-speed stability. The Owl airfoil offers clear advantages for endurance missions, with its minimal drag translating to significantly longer flight times or lighter propulsion demands. While the Falcon provides niche benefits in drag reduction, both the Eppler 387 and NACA 4412 were conclusively outperformed, underscoring the limitations of conventional airfoils in low-Reynolds UAV applications. Overall, this research confirms that bio-inspired geometries outperform fixed conventional designs, directly supporting the objective of leveraging morphing winglets as a pathway to drag reduction and aerodynamic efficiency improvement in next-generation commercial aircraft.

Funding Declaration

This research did not receive any specific grant from funding agencies in the public, commercial, or not-for-profit sectors.

Clinical Trial Number: Not applicable.

Declarations

Ethics Approval and Consent to Participate:

Not applicable.

Consent for publication:

Not applicable.

Competing interests:

The authors declare that they have no competing interests.

Authors' Contributions:

All authors read and approved the final manuscript.

Acknowledgments:

Not applicable.

References

Xia, J. (2024). Fluid dynamics study on flight performance improvement of morphing winglets on jetliners. *In Proceedings of the 4th International Conference on Materials Chemistry and Environmental Engineering* (*Applied and Computational Engineering*, *59*, 199–203). https://doi.org/10.54254/2755-2721/59/20240802

Clements, D. (2023). *Effects of morphing wings on aerodynamic performance and energy efficiency improvement for ground effect vehicles* (Doctoral thesis, University of Southampton). https://eprints.soton.ac.uk/478220/

Özel, C., Özbek, E., & Ekici, S. (2020). A review on applications and effects of morphing wing technology on UAVs. *International Journal of Aviation Science and Technology, 1*(1), 30–40. https://doi.org/10.23890/IJAST.vm01is01.0105

Eguea, J. P., Bravo-Mosquera, P. D., & Catalano, F. M. (2021). Camber morphing winglet influence on aircraft drag breakdown and tip vortex structure. *Aerospace Science and Technology, 119*, 107148. https://doi.org/10.1016/j.ast.2021.107148

Samuel, A. A., Badmus, O., Iheuwa, G. O., Ehizojie, L., & Segun, S. E. (2025). Comparative analysis of GitOps tools and frameworks. *Path of Science: International Electronic Scientific Journal, 11*(5), 117–9. https://doi.org/10.22178/pos.117-9

Kaygan, E. (2020). Aerodynamic analysis of morphing winglets for improved commercial aircraft performance. *Journal of Aviation, 4*(1), 31–44. https://doi.org/10.30518/jav.716194

Eguea, J. P., Da Silva, G. P. G., & Catalano, F. M. (2020). Fuel efficiency improvement on a business jet using a camber morphing winglet concept. *Aerospace Science and Technology, 96*, 105542. https://doi.org/10.1016/j.ast.2019.105542

Gavrilović, N. N., Rašuo, B. P., Dulikravich, G. S., & Parezanović, V. B. (2015). Commercial aircraft performance improvement using winglets. *FME Transactions, 43*(1), 1–8. https://doi.org/10.5937/fmet1501001G

Ursache, N., Melin, T., Isikveren, A., & Friswell, M. (2007). Morphing winglets for aircraft multi-phase improvement. *In Proceedings of the 7th AIAA Aviation Technology, Integration, and Operations Conference; 2nd CEIAT International Conference on Innovation and Integration in Aero Sciences; 17th Lighter-Than-Air Systems Technology Conference; and 2nd TEOS Forum* (Paper No. 2007-7813). American Institute of Aeronautics and Astronautics. https://doi.org/10.2514/6.2007-7813

Eguea, J. P., Bravo-Mosquera, P. D., & Catalano, F. M. (2021). Camber morphing winglet influence on aircraft drag breakdown and tip vortex structure. *Aerospace Science and Technology, 119*, 107148. https://doi.org/10.1016/j.ast.2021.107148

Liauzun, C., Le Bihan, D., David, J. M., Joly, D., & Paluch, B. (2018). Study of morphing winglet concepts aimed at improving load control and the aeroelastic behavior of civil transport aircraft. *Journal of Aerospace Lab*, (14), 1–15. https://aerospacelab.onera.fr/sites/default/files/2024-01/AL14-10_0.pdf

Wang, W., & Yuan, G. (2024). Review on the structure design of morphing winglets. *Aerospace*, 11(12), 1004. https://doi.org/10.3390/aerospace11121004

Rajabi, M., & Jahangirian, A. (2024). Design optimization of a morphing winglet for all flight missions of a civil aircraft. *Proceedings of the Institution of Mechanical Engineers, Part G: Journal of Aerospace Engineering, 239*(3), 209–222. https://doi.org/10.1177/09544100241287653

Popov, V., Loginov, V., Shmyrov, V., Ukrainets, Y., Steshenko, P., & Hlushchenko, P. (2020). Improving aircraft fuel efficiency by using the adaptive wing and winglets. *Eastern-European Journal of Enterprise Technologies*, 2(1), 104. https://doi.org/10.15587/1729-4061.2020.200664

Segun, S. E., Oluwafunke, O. A., Iyase, O. L., Aransiola, E. A., Adeagbo, M. A., Abisola, B. A., & Dada, B. J. (2023). An automatic traffic violation ticketing system using radio frequency identification (RFID) technology. *Journal of Engineering Research and Reports, 25*(1), 61–69. https://doi.org/10.9734/jerr/2023/v25i1870

Dimino, I., Andreutti, G., Moens, F., Fonte, F., Pecora, R., & Concilio, A. (2021). Integrated design of a morphing winglet for active load control and alleviation of turboprop regional aircraft. *Applied Sciences, 11*(5), 2439. https://doi.org/10.3390/app11052439

Tang, H., Zhang, W., Cao, J., Cao, Y., Bi, X., Zhao, H., Zhang, Z., Liu, Z., Wan, T., Lang, R., Sun, W., Du, S., Yang, Y., Lu, Y., Zeng, D., Wu, J., Duan, B., Lin, D., Li, F., … Editorial Board of the Chinese Journal of Hepatobiliary Surgery. (2025). Chinese expert consensus on sequential surgery following conversion therapy based on combination of immune checkpoint inhibitors and antiangiogenic targeted drugs for advanced hepatocellular carcinoma (2024 edition). *Bioscience Trends, 18*(6), 505–524. https://doi.org/10.5582/bst.2024.01394

Ajayi, A. S., Kim, S., & Yun, R. (2024). Study of developing a condensation heat transfer coefficient and pressure drop model for whole reduced pressure ranges. *International Journal of Air-Conditioning and Refrigeration, 32*, 15. https://doi.org/10.1007/s44189-024-00060-0

Yusoff, H., Koay, M. H., Ghaffar, H., Mohd Yamin, A. F., Ramli, M. R., Wan Mohamed, W. M., & Mohd Halidi, S. N. A. (2022). The evolution of induced drag of multi-winglets for aerodynamic performance of NACA23015. *Journal of Advanced Research in Fluid Mechanics and Thermal Sciences, 93*(2), 100–110. https://doi.org/10.37934/arfmts.93.2.100110

Madani, S. A. S., Vaezi, E., & Keshmiri, A. (2025). CFD-driven evaluation of winglet cant angle: Insights into aerodynamic and aeroacoustic performance. *Results in Engineering, 26*, 104759. https://doi.org/10.1016/j.

rineng.2025.104759

Reist, T. A., Koo, D., & Zingg, D. W. (2022). Aircraft cruise drag reduction through variable camber using existing control surfaces. *Journal of Aircraft*, 59(6), 1406–1415. https://doi.org/10.2514/1.C036754

Fasasi, S. T., Ajifowowe, I., Adeyemo, A., & Ajayi, A. (2024). Development of an expert system for aircraft failures causes, predictions, and remedies. *International Journal of Aerospace Engineering (IJASE), 2*(1), 12–20. https://iaeme.com/MasterAdmin/Journal_uploads/IJASE/VOLUME_2_ISSUE_1/IJASE_02_01_002.pdf

Shahid, F., Alam, M., Park, J.-Y., Choi, Y., Park, C.-J., Park, H.-K., & Yi, C.-Y. (2025). Bioinspired morphing in aerodynamics and hydrodynamics: Engineering innovations for aerospace and renewable energy. *Biomimetics, 10*(7), Article 427. https://doi.org/10.3390/biomimetics10070427

Bishay, P. L., Brody, M., Podell, D., Corte-Garcia, F., Muñoz, E., Minassian, E., & Bradley, K. (2023). 3D-printed bio-inspired mechanisms for bird-like morphing drones. *Applied Sciences, 13*(21), 11814. https://doi.org/10.3390/app132111814